



ELSEVIER

Signal Processing 80 (2000) 2527–2540

**SIGNAL
PROCESSING**

www.elsevier.nl/locate/sigpro

New methods of radar performances analysis

E. Jay^{a,b,*}, J.-P. Ovarlez^b, P. Duvaut^a

^aENSEA/UCP-ETIS, URA D2235, BP 44, F95014 Cergy Pontoise, Cedex, France

^bONERA, DEMR/TSI, BP72, F92322 Châtillon, Cedex, France

Received 29 July 1999; received in revised form 6 June 2000

Abstract

Original methods for radar detection performance analysis are derived for a fluctuating or non-fluctuating target embedded in additive and a priori unknown noise. This kind of noise can be, for example, the sea or ground clutter encountered in surface-based radar for the detection of low grazing angle targets and/or in high-resolution radar. In these cases, the spiky clutter tends to have a statistic which strongly differs from the Gaussian assumption. Therefore, the detection theory is no longer appropriate since the nature of statistics has to be known. The new methods proposed here are based on the parametric modelling of the moment generating function of the noise envelope by Padé approximation, and lead to a powerful estimation of its probability density function. They allow to evaluate the radar detection performances of targets embedded in arbitrary noise without knowledge of the closed form of its statistic and in the same way to take into account any possible fluctuation of the target. These methods have been tested successfully on synthetic signals and used on experimental signals such as ground clutter. © 2000 Elsevier Science B.V. All rights reserved.

Zusammenfassung

Typische Methoden zur Analyse der Eigenschaften von Radardetektoren sind für bewegte und nicht-bewegte Ziele in additivem und a priori unbekanntem Rauschen hergeleitet worden. Derartiges Rauschen kann beispielsweise als See- oder Bodenclutter im oberflächen-basierten Radar für die Detektion von Zielen mit kleinen *grazing angles* und/oder beim hochauflösenden Radar angetroffen werden. In diesen Fällen tendiert das mit Spitzen versehene *clutter* zu einer Statistik, die sich von einer angenommenen Gaußverteilung nachhaltig unterscheidet. Demzufolge sind die theoretischen Betrachtungen zur Detektion aufgrund der unbekanntenen statistischen Eigenschaften nicht mehr geeignet. Die hier vorgestellten neuen Methoden basieren auf der parametrischen Modellierung der momentenerzeugenden Funktion mit Hilfe der Pade Approximation und führen zu einer leistungsstarken Schätzung der Wahrscheinlichkeitsdichtefunktion. Diese Methoden gestatten die Überprüfung des Detektionsverhaltens bei Zielen im Umgebungsrauschen ohne Kenntnis der Statistik in geschlossener Form und unter Berücksichtigung jeglicher Quellenfluktuation. Tests mit synthetischen Signalen wurden erfolgreich mit diesen Methoden durchgeführt und auf experimentelle Signale, wie Bodenclutter angewendet. © 2000 Elsevier Science B.V. All rights reserved.

Résumé

De nouvelles méthodes d'analyse de performances de détection radar sont présentées dans le cadre d'une cible fluctuante ou non noyée dans un bruit additif a priori inconnu. Ce type de bruit peut être, par exemple, du fouillis de mer ou de sol rencontré dans le cadre de la détection de cible à site bas et/ou pour un radar à haute résolution distance; la nature impulsionnelle d'un tel fouillis écarte l'hypothèse gaussienne généralement retenue pour la modélisation de sa

* Correspondence address: ONERA, DEMR/TSI, BP72, F92322 Châtillon, Cedex, France.

E-mail address: jay@onera.fr (E. Jay).

statistique. Les nouvelles méthodes proposées ici se basent sur la modélisation paramétrique de la fonction génératrice de moments de l'enveloppe du bruit par approximants de Padé et conduisent à une estimation de sa densité de probabilité. Elles permettent d'évaluer les performances de détection radar d'une cible noyée dans un bruit quelconque sans connaissance de sa statistique et permettent, de la même manière, de prendre en compte toute fluctuation éventuelle de la cible. Ces méthodes ont été testées avec succès sur signaux synthétiques et ont été mises en œuvre sur signaux réels, tel que du fouillis de forêt. © 2000 Elsevier Science B.V. All rights reserved.

Keywords: Radar detection; Performance analysis; Signal noise

1. Description of the problem

The radar detection of a target against a background of unwanted clutter due to echoes from sea or land is a problem of interest in the radar field. For many years, the statistics of quadrature components of the radar clutter were supposed to be jointly Gaussian because of the low radar resolution capabilities: in this case, the clutter was viewed as a sum of echoes from a very large number of elementary scatterers (Central Limit Theorem). Current systems have now improved their resolution capabilities and hence their detection performance. However, as resolution is increased, the statistics of the additive noise is no longer Gaussian. Recent experimentations conducted at ONERA and other organizations like MIT [5] indicate that large deviations from Rayleigh statistics are observed in situations such as low grazing angle illumination and/or high resolution. In such cases, due to the spiky nature of the clutter, the empirical distribution exhibits both higher tails and larger standard deviation relative to the mean than predicted by the Rayleigh distribution. Therefore, many work has been devoted to fit empirical models of distribution to experimental data. This is the case of the compound Gaussian processes [8,9], also called spherically invariant random processes (SIRP) which allow to model the multivariate probability density function (PDF) of the envelope of the clutter returns, taking into account the possible spatial or temporal correlation of the processes. The well-known log-normal, Weibull and K -distribution densities [6] belong to this class of distributions but the main problems with this kind of approach are the quality of the estimation of the SIRP parameters and the complexity of the optimal detector implementation. In this paper, we propose

to analyze the performances of radar detection of a target embedded in any combination of clutter and thermal noise without knowledge of the closed form of noise densities. The estimation of the noise envelope density is only performed according to the modelisation with Padé approximation of the moment generating function (MGF) for the noise envelope. This method is based on the estimation of all n -order moments of the noise envelope, which we will suppose exactly estimated. This kind of modelisation allows to derive, for a constant false alarm rate, the simple form of the detection probability (P_d) of a target with constant or fluctuating envelope embedded in a complex noise fully characterized by the moments of its envelope.

2. General relations of the detection theory

2.1. Neymann–Pearson criterion

We consider here the basic problem of detecting the presence or absence of a complex signal $s(t)$ with envelope A in a set of measurements $y(t) = y_1(t) + iy_2(t)$ corrupted by a sum of independent additive complex noise signals $c(t)$ corresponding to the clutter echoes and white Gaussian thermal noise. This problem can be described mathematically in terms of a test between the following pair of statistical hypothesis, where $c(t)$ denotes all the unwanted noises:

$$\text{Hypothesis } H_0: y(t) = c(t), \quad (1)$$

$$\text{Hypothesis } H_1: y(t) = s(t) + c(t). \quad (2)$$

The Neymann–Pearson criterion fixes the probability of false alarm P_{fa} and maximizes the probability to detect signal P_d over the detection threshold θ depending on the P_{fa} value.

2.2. Statistical framework

Throughout this paper, we consider the *Envelope Detection* scheme of the complex signal $y(t)$. In a statistic framework, expressions of P_d and P_{fa} need to be derived and depend on the noise envelope statistic characterized by its probability density function (PDF). If we note $p_{H_0}(r)$ the probability density of the noise envelope $|c(t)|$ under H_0 hypothesis, the detection threshold θ is fixed by the value of the given probability of false alarm P_{fa} :

$$P_{fa} = \int_{\theta}^{+\infty} p_{H_0}(r) dr. \tag{3}$$

While denoting $p_{H_1}(r)$ the PDF of the envelope of the complex signal embedded in noise $|s(t) + c(t)|$ under H_1 hypothesis, the detection probability P_d is fully characterized by

$$P_d = \int_{\theta}^{+\infty} p_{H_1}(r) dr. \tag{4}$$

Since phases between quadrature components of the clutter, thermal noise and target are unknown, they are commonly supposed to be uniformly distributed on $[-\pi, \pi]$. This hypothesis is very important because in this case, each two-dimensional density function of the quadrature component is hence a circular symmetric distribution. So we can find [7] a very interesting relation between the PDF of the noise plus signal envelope ($p_{H_1}(r;A)$) and the PDF of the noise envelope ($p_{H_0}(r)$), using the coherent radial characteristic function of the noise process.

2.3. Basic relation

Let us consider a random complex process with real part $a(t)$ and imaginary part $b(t)$. This process is characterised by its two-dimensional density function $p(a, b)$, or dually, by a so-called *coherent* characteristic function $C(u_1, u_2)$, which is $p(a, b)$ Fourier transform:

$$C(u_1, u_2) = \iint_{-\infty}^{+\infty} p(a, b) e^{i(u_1 a + u_2 b)} da db. \tag{5}$$

This characteristic function can be transformed in a single radial variate ρ function (ρ represents the

value of the signal envelope, $\rho = \sqrt{u_1^2 + u_2^2}$) with the assumption of a phase uniformly distributed i.e. $p_{\phi}(\alpha = \arctan(b/a)) = 1/2\pi$, independent of the envelope $p_r(r = \sqrt{a^2 + b^2})$. So we have

$$p(a, b) da db = p_{\phi}(\alpha)p_r(r) d\alpha dr, \tag{6}$$

and

$$\begin{aligned} C(\rho) &= \int_0^{2\pi} p_{\phi}(\alpha) \left[\int_0^{+\infty} p_r(r) e^{i\rho r \cos \alpha} dr \right] d\alpha \\ &= \int_0^{+\infty} p_r(r) \left[\frac{1}{2\pi} \int_0^{2\pi} e^{i\rho r \cos \alpha} d\alpha \right] dr, \end{aligned}$$

i.e.

$$C(\rho) = \int_0^{+\infty} p_r(r) J_0(\rho r) dr, \tag{7}$$

where $J_0(x)$ denotes the ordinary Bessel function of order 0. Inverting expression (7), we obtain $p_r(r)$ as a function of $C(\rho)$:

$$p_r(r) = \int_0^{+\infty} r\rho C(\rho) J_0(\rho r) d\rho. \tag{8}$$

In the following, the next two results will be used:

- For a signal with constant envelope A and an uniform phase, the PDF is characterised by

$$p(r) = \delta(r - A),$$

where $\delta(\cdot)$ is the Dirac distribution, and the coherent radial characteristic function is given by

$$C(\rho) = J_0(\rho A).$$

- The characteristic function $C_{H_1}(\rho)$ of the sum of the signal $s(t)$ and unwanted clutter $c(t)$, is equal to the product of the characteristic functions of signal $C_s(\rho)$ and of noise $C_c(\rho)$.

It is now possible to derive a relation between the density $p_{H_0}(r)$ of the envelope under hypothesis H_0 (noise only) and the density $p_{H_1}(r;A)$ of the envelope under hypothesis H_1 (noise and signal with constant envelope A), recalling that the following results are derived under the strong hypothesis of uniform phases distributions between the in-phase and quadrature components of each

process:

$$\begin{aligned} p_{H_1}(r;A) &= \int_0^{+\infty} r\rho C_s(\rho)C_c(\rho)J_0(\rho r) d\rho \\ &= \int_0^{+\infty} r\rho J_0(\rho A)C_c(\rho)J_0(\rho r) d\rho, \end{aligned} \quad (9)$$

with

$$C_c(\rho) = \int_0^{+\infty} p_{H_0}(r)J_0(\rho r) dr. \quad (10)$$

Replacing (10) in (9) leads to the following important relation:

$$\begin{aligned} p_{H_1}(r;A) &= \int_0^{+\infty} \int_0^{+\infty} r\rho J_0(\rho A)J_0(\rho r) \\ &\quad \times J_0(\rho r')p_{H_0}(r') d\rho dr'. \end{aligned} \quad (11)$$

In the case of fluctuating target with envelope density fluctuation law $p(A;A_0)$ (where A_0 represents the mean value of the fluctuations), relation (11) becomes more general:

$$\begin{aligned} p_{H_1}(r;A_0) &= \int_0^{+\infty} p_{H_1}(r;A)p(A;A_0) dA \\ &= \int_0^{+\infty} \int_0^{+\infty} r\rho J_0(\rho r)J_0(\rho r')p_{H_0}(r') \\ &\quad \times \left[\int_0^{+\infty} J_0(\rho A)p(A;A_0) dA \right] d\rho dr'. \end{aligned} \quad (12)$$

This relation is very important because it shows that all the expressions needed to evaluate the detection performances are related to the noise envelope statistic $p_{H_0}(r)$.

Example 1 (Gaussian noise). *Non-fluctuating target*: Relation (11) connects the PDF of the envelope of a complex Gaussian noise, i.e. a Rayleigh distribution (power $2\sigma^2$):

$$p_{H_0}(r) = \frac{r}{\sigma^2} \exp\left(-\frac{r^2}{2\sigma^2}\right), \quad (13)$$

to the envelope PDF of a constant signal embedded in this complex noise, which leads to the well

known Rice–Nakagami distribution:

$$p_{H_1}(r;A) = \frac{r}{\sigma^2} \exp\left(-\frac{A^2 + r^2}{2\sigma^2}\right) I_0\left(\frac{rA}{\sigma^2}\right), \quad (14)$$

where $I_0(x)$ is the modified Bessel function of the first kind and zero order. Replacing (14) in (4) gives a first expression of P_d for a non-fluctuating target embedded in complex Gaussian noise:

$$P_d = \int_0^{+\infty} p_{H_1}(r;A) dr = \mathcal{Q}\left(\frac{A}{\sigma}, \frac{\theta}{\sigma}\right), \quad (15)$$

where $\mathcal{Q}(a, b)$ is the Marcum \mathcal{Q} -function defined by

$$\mathcal{Q}(a, b) = \int_b^{+\infty} x \exp\left(-\frac{x^2 + a^2}{2}\right) I_0(ax) dx \quad (16)$$

and the detection threshold θ obtained for a given P_{fa} according to (3) and (13):

$$\theta = \sqrt{-2\sigma^2 \log(P_{fa})}. \quad (17)$$

Fluctuating target: If the target is fluctuating according to a Swerling I law of power A_0^2 ,

$$p(A;A_0) = \frac{2A}{A_0^2} \exp\left(-\frac{A^2}{A_0^2}\right) \quad (18)$$

relation (12) becomes

$$p_{H_1}(r;A_0) = \frac{2r}{2\sigma^2 + A_0^2} \exp\left(-\frac{r^2}{2\sigma^2 + A_0^2}\right), \quad (19)$$

which corresponds to a Rayleigh distribution with power $2\sigma^2 + A_0^2$. Then we have (θ is derived according to (17)):

$$\begin{aligned} P_d &= \int_0^{+\infty} p_{H_1}(r;A_0) dr \\ &= \exp\left(-\frac{\theta^2}{2\sigma^2 + A_0^2}\right). \end{aligned} \quad (20)$$

Example 2 (K -distributed noise and non-fluctuating target). The K -distributed noise envelope is K -distributed with probability density function

(PDF):

$$p_{H_0}(r) = \frac{b^{v+1}}{2^{v-1}\Gamma(v)} r^v K_{v-1}(br), \quad (21)$$

cumulative density function (CDF)

$$F(r) = 1 - \frac{(br)^v}{\Gamma(v)2^{v-1}} K_v(br), \quad (22)$$

and coherent radial characteristic function

$$C(\rho) = \frac{1}{(1 + \rho^2/b^2)^v}, \quad (23)$$

where $K_v(\cdot)$ is the modified Bessel function of the third kind, v is the shape of the density and parameter b is related to the second-order moment σ^2 by:

$$b = 2\sqrt{\frac{v}{\sigma^2}}. \quad (24)$$

Smaller is the value of the shape parameter v , spikier is the K -distribution and when $v \rightarrow +\infty$, it is close to a Gaussian distribution.

Relation (11) becomes in this case

$$p_{H_1}(r;A) = \int_0^{+\infty} r\rho \frac{J_0(\rho A)J_0(\rho r)}{(1 + \rho^2/b^2)^v} d\rho.$$

In order to derive the expression of P_d we just have to integrate the above expression with respect to r . Using the tables [1] this expression becomes

$$P_d = 1 - \int_0^{+\infty} \theta \frac{J_0(\rho A)J_1(\rho\theta)}{(1 + \rho^2/b^2)^v} d\rho. \quad (25)$$

The expression of the threshold θ is detailed further in (46).

The two relations (11) and (12) are usually quite difficult to compute numerically for evaluating the detection performances for several signal-to-noise ratios.

In the next section, we will use an interesting method proposed and developed in [2–4] which allows to estimate the PDF of any noise from its n -order moments and give very useful relations to compute the pair P_d, P_{fa} for a given signal-to-noise ratio. This method is described in the following section in a general way, and then applied to the detection performance analysis.

3. Padé approximation

3.1. Description of the method

This method [2–4] is based on the parametric construction of the moment generating function (MGF) of the noise envelope by Padé approximation. The MGF $\Phi(u)$ of a random process is defined by the mono-lateral Laplace transform of its envelope PDF $p(r)$:

$$\Phi(u) = \int_0^{+\infty} p(r) e^{-ur} dr. \quad (26)$$

After a Taylor series expansion of e^{-ur} around $u = 0$, $\Phi(u)$ can be expressed as follows:

$$\Phi(u) = \sum_{n=0}^{\infty} \mu_n \frac{(-u)^n}{n!} = \sum_{n=0}^{\infty} c_n u^n, \quad u \rightarrow 0, \quad (27)$$

where $\mu_n = \int_0^{+\infty} r^n p(r) dr$ denotes the n th-order moments of the process envelope.

If we assume all the moments μ_n perfectly known up to order $L + M + 1$, the main idea is to truncate the infinite series at the order $L + M + 1$ and to approximate it by a rational function $P^{[L/M]}(u)$ ($L \leq M$) defined by

$$P^{[L/M]}(u) = \frac{\sum_{n=0}^L a_n u^n}{\sum_{n=0}^M b_n u^n}, \quad (28)$$

where the coefficients $\{a_n\}$ and $\{b_n\}$ are determined so that the following relation is verified:

$$\frac{\sum_{n=0}^L a_n u^n}{\sum_{n=0}^M b_n u^n} = \sum_{n=0}^{L+M} c_n u^n + \mathcal{O}(u^{L+M+1}). \quad (29)$$

The notation $\mathcal{O}(u^{L+M+1})$ simply takes into account terms of order higher than u^{L+M} . To determine the two sets of coefficients $\{a_n\}$ and $\{b_n\}$, we have to match the coefficients:

$$\sum_{n=0}^M b_n u^n \sum_{n=0}^{L+M} c_n u^n = \sum_{n=0}^L a_n u^n + \mathcal{O}(u^{L+M+1}). \quad (30)$$

The moments matching conditions fix in a first step the set of coefficients $\{b_n\}$ by solving a simple set of M linear equations for the M unknown denominator coefficients:

$$\sum_{n=0}^M b_n c_{L-n+j} = -c_{L+j}, \quad 1 \leq j \leq M \quad (31)$$

which can be written as matrix and linear system,

$$\begin{pmatrix} c_{L-M+1} & \cdots & c_L \\ \vdots & \vdots & \vdots \\ c_{L-M+k} & \cdots & c_{L+k-1} \\ \vdots & \vdots & \vdots \\ c_L & \cdots & c_{L+M-1} \end{pmatrix} \mathbf{b} = -\mathbf{c}, \quad (32)$$

where $\mathbf{b} = (b_M, \dots, b_k, \dots, b_1)^T$, and $\mathbf{c} = (c_{L+1}, \dots, c_{L+k+1}, \dots, c_{L+M})^T$.

In a second step the set $\{a_n\}$ is determined by a simple convolution of the $\{b_n\}$ and the $\{c_n\}$ coefficients:

$$a_j = c_j + \sum_{i=1}^j b_i c_{j-i}, \quad 0 \leq j \leq L. \quad (33)$$

The set of coefficients $\{a_n\}$ and $\{b_n\}$ determined from (32) and (33), defines, owing to the Padé Approximation, the *One Point* parametric modelling of the MGF given its power series expansion (27) at $u = 0$.

If we suppose that the rational fraction approximation has M distinct poles with negative real part to assure its convergence for $u \rightarrow \infty$, relation (28) can be rewritten as

$$P^{[L/M]}(u) = \sum_{k=1}^M \frac{\lambda_k}{u - \alpha_k}, \quad \text{Re}(\alpha_k) < 0. \quad (34)$$

From this description, we are able to determine a random vector PDF and CDF using the inverse Laplace transform of the corresponding MGF performed by residue inversion formula and leading to a sum of weighted decaying complex exponentials.

3.2. PDF and CDF expressions

We saw (26) that MGF is the PDF Laplace transform. Using the inversion residue formula on (34) results in approximate PDF and CDF as a sum of weighted decaying complex exponentials:

$$p(r) = \sum_{k=1}^M \lambda_k e^{\alpha_k r}, \quad \text{Re}(\alpha_k) < 0, \quad (35)$$

$$F(r) = 1 + \sum_{k=1}^M \frac{\lambda_k}{\alpha_k} e^{\alpha_k r}. \quad (36)$$

Given the moments of a random process, the tail of the PDF is more accurately approximated, that is, the region $u \rightarrow 0$ in $\Phi(u)$ corresponds to $r \rightarrow \infty$ in $p(r)$. This is the reason why such approximations are very interesting in radar detection studies for the P_d and P_{fa} computations (needing PDF tails integration).

The Padé approximation yields good results in the estimation of a PDF and an example is shown in Fig. 1 for the K -distribution PDF defined by (21) with $\nu = 0.1$, $\sigma^2 = 1$ and b related to ν and σ^2 by (24). The relative error ϵ_{rel} is defined as follows:

$$\epsilon_{rel} = \left| \frac{K_{approx} - K_{theo}}{K_{theo}} \right|. \quad (37)$$

3.3. Extension

- *Variates generation:* As we now know the expression of a random variate CDF (36), we can generate samples X according to (35) as follows:

1. Generate $U \sim \mathcal{U}[0,1]$.
2. Generate $X \sim F^{-1}(U)$.

In our case these generated samples represent variates envelope. As ones can write for a random complex process Z that $Z = |Z|e^{j\Phi}$ (where Φ is the assumed uniform phase between the I and Q components of the process), the complex process can be retrieved in generating Φ as an uniformly distributed variate in $[0,2\pi]$. This could be useful in the case where only data envelope are available.

- *Two-points approximation:* To obtain a more uniform approximation, we could use a two-points approximation, often about $u \rightarrow 0$ and $u \rightarrow +\infty$. This requires that the MGF be investigated in the vicinity of these two points, and not surprisingly $u \rightarrow +\infty$ in $\Phi(u)$ implies $r \rightarrow 0$ in $p(r)$. We will not use the two-points Padé approximation in this paper because our goal is to apply the method to detect problems that principally require the study of the tail of the distribution and because of the lack of knowledge about the Markov coefficients needed in the expansion at $u \rightarrow +\infty$ (see [2] for more details).
- *Stabilization:* In the case where some poles have positive real part, it is necessary to stabilize the rational fraction without changing the moments.

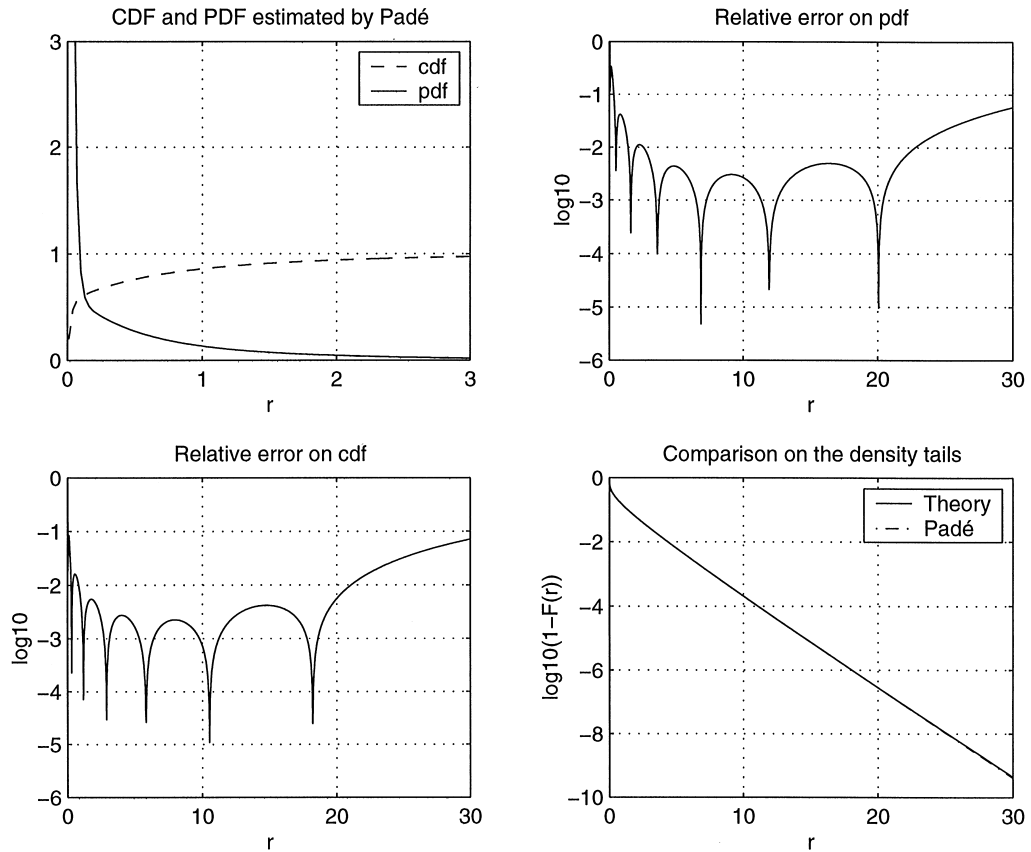


Fig. 1. Analysis of Padé K -distribution approximation ($\nu = 0.1$) and ($\sigma^2 = 1$).

Such a stabilization procedure is proposed in [2]. The task is to find a new approximation that is stable and does not sacrifice the original and extrapolated moments. This consists in rewriting the moments expression in terms of the residues and the poles and looking for the smallest change necessary to make the unstable approximation a stable one (i.e. singularities of the MGF in the left-half plane). But any change on the residues and the poles perturbs the moments and a compromise between the two effects has to be found.

In this work, we do not use this kind of procedure. A first choice for the order of the numerator L and the denominator M is $L = M - 1$. This assures the convergence of the MGF when $|u| \rightarrow +\infty$ and the resulting approximation called *sub-diagonal* is known to be one of the more accu-

rate (with *diagonal* approximation where $L = M$). The second choice to find the value of M is to test the negativity of the poles. The initialised value of M is set to be equal to an upper value K (so $L = K - 1$) and we compute the poles and residues values. If the poles satisfy the real part negativity condition, then the approximation is found. Otherwise, we change the value of M to $M - 1$ (L to $L - 1$) and compute the new residues and poles values testing the sign of the real part of the poles. The upper value K is determined according to the rank of the Hankel matrix in (32) which is not always full (in this case the rank is full when equal to M). So we look for the highest value K which coincides with M among all the rank values coinciding with M (varying from 1 to 15). It means that for $M \geq K$ the rank is deficient.

3.4. Comparison with another method

This method has to be compared with a non-parametric method, based on the PDF estimation by a kernel method described in [10]. However, this one is not well adapted to our problem because of its poor quality of estimation in the tail of distribution. The mismatch of this last method can be seen in Fig. 2 where the kernel estimated PDF of the *K*-distribution ($\nu = 0.1$) is plotted. The relative error shows the non-efficiency of the kernel estimation if applied to our task.

In the next section, we use the method to approximate the noise PDF (that allows to simply determine the detection threshold value with wanted P_{fa}) and to take into account the target fluctuations which PDF will be also estimated by Padé approximation.

4. Evaluation of detection performances

General relations given by (11) and (12) can be simplified when using Padé approximations for the noise envelope and envelope fluctuation PDF. With the knowledge of the noise envelope of the experimental data, $p_{H_0}(r)$ can be approximated using (35):

$$p_{H_0}(r) = \sum_{k=1}^M \lambda_k e^{\alpha_k r}, \tag{38}$$

where the set of coefficients $\{\lambda_k\}$ and $\{\alpha_k\}$ is determined by the Padé approximation. So, the detection threshold θ is perfectly defined by the determination (Newton find root algorithm) of the non-linear equation (see (3)):

$$P_{fa} = - \sum_{k=1}^M \frac{\lambda_k}{\alpha_k} e^{\alpha_k \theta}. \tag{39}$$

4.1. Non-fluctuating target

We always suppose that the constant envelope of the target is $|s(t)| = A$. Using (38) in (11) leads to

$$p_{H_1}(r;A) = \int_0^{+\infty} \rho J_0(\rho A) J_0(\rho r) \sum_{k=1}^M \frac{\lambda_k}{\sqrt{\rho^2 + \alpha_k^2}} d\rho. \tag{40}$$

Recalling, owing to [1], that

$$\int_0^\theta r J_0(\rho r) dr = \theta J_1(\rho \theta) / \rho,$$

$$\int_0^{+\infty} J_0(\rho y) e^{\alpha_k y} dy = \frac{1}{\sqrt{\rho^2 + \alpha_k^2}},$$

the detection probability P_d defined by (4) takes the simple form

$$P_d = 1 - \int_0^{+\infty} \theta J_0(\rho A) J_1(\rho \theta) \sum_{k=1}^M \frac{\lambda_k}{\sqrt{\rho^2 + \alpha_k^2}} d\rho, \tag{41}$$

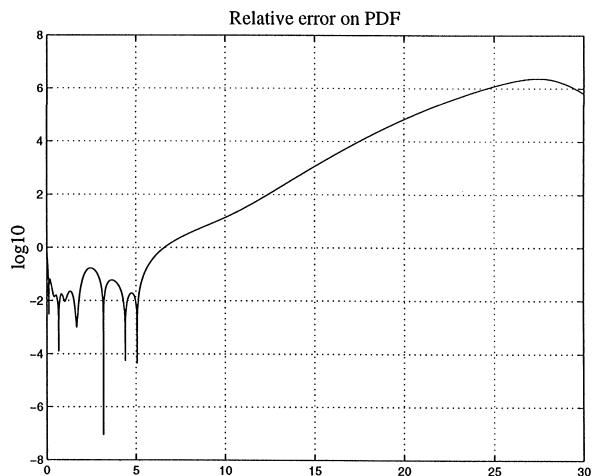
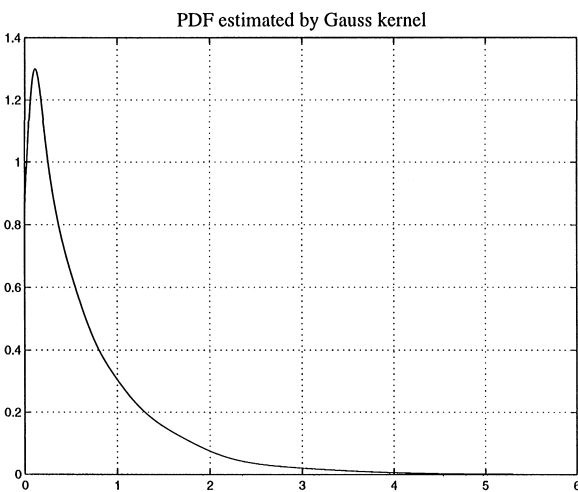


Fig. 2. Analysis of Gaussian kernel *K*-distribution PDF estimation ($\nu = 0.1$) and ($\sigma^2 = 1$).

where the detection threshold θ is perfectly defined by the determination of (39).

4.2. Fluctuating target

In the case of fluctuating target (Swerling fluctuations for example), it is possible to estimate the envelope fluctuation density $p(A;A_0)$ (where A_0 is mean value of fluctuation) by Padé approximation:

$$p(A;A_0) = \sum_{i=1}^N \frac{\gamma_i}{A_0} e^{(\delta_i/A_0)A}, \tag{42}$$

where the N parameters $\{\gamma_i\}$ and $\{\delta_i\}$ are once determined when $A_0^2 = 1$. Eq. (12) can be transformed as

$$p_{H_1}(r;A_0) = \int_0^{+\infty} r\rho J_0(\rho r) \sum_{k=1}^M \frac{\lambda_k}{\sqrt{(\rho^2 + \alpha_k^2)}} \times \sum_{i=1}^N \frac{\gamma_i}{\sqrt{(\rho^2 A_0^2 + \delta_i^2)}} d\rho \tag{43}$$

which leads to the detection probability formula with the detection threshold θ always given by the resolution of (39):

$$P_d = 1 - \int_0^{+\infty} \theta J_1(\rho\theta) \sum_{k=1}^M \frac{\lambda_k}{\sqrt{(\rho^2 + \alpha_k^2)}} \times \sum_{i=1}^N \frac{\gamma_i}{\sqrt{(\rho^2 A_0^2 + \delta_i^2)}} d\rho. \tag{44}$$

Relations (41) and (44) are very general and can be easily computed, since we have therefore only one integration to compute instead of quadruple generalized integration without Padé approximation. The latter allows to evaluate any radar detection performance for any target embedded in any noise.

Successful tests of this method on synthetic signals allow us to be optimistic for the evaluation of PDF and CDF Padé approximation obtained on experimental forest clutter data and of their radar detection performance that we perform in the next section. We show, according to these results, the mismatch between the real hypothesis and the Rayleigh hypothesis.

5. Some results

5.1. Synthetic signals

We choose K -distributed clutter (power $\sigma^2 = 1$), as described in (21), with a small shape parameter $\nu = 0.1$ and a parameter b given by (24). Fig. 3 shows some realisations of K -distributed processes with different values of the shape parameter $\nu = 0.1, 2, 10, +\infty$ ($\nu = +\infty$ corresponds to a Rayleigh process) and power $\sigma^2 = 1$. The associated coherent radial characteristic function is

$$C(\rho) = \left(1 + \frac{\rho^2}{b^2}\right)^{-\nu}. \tag{45}$$

Detection threshold θ is defined by the determination of the non-linear equation

$$P_{fa} = \frac{(b\theta)^\nu}{\Gamma(\nu)2^{\nu-1}} K_\nu(b\theta), \tag{46}$$

and so, for a non-fluctuating target we first have

$$P_d = 1 - \int_0^{+\infty} \theta \frac{J_0(\rho A) J_1(\rho\theta)}{(1 + \rho^2/b^2)^\nu} d\rho. \tag{47}$$

If we consider the target fluctuations with a Swerling I probability law (variance A_0^2),

$$p(A;A_0) = \frac{2A}{A_0^2} \exp\left(-\frac{A^2}{A_0^2}\right), \tag{48}$$

Eq. (47) becomes

$$P_d = 1 - \int_0^{+\infty} \theta \frac{J_1(\rho\theta) e^{-\rho^2 A_0^2/4}}{(1 + \rho^2/b^2)^\nu} d\rho. \tag{49}$$

Fig. 4 shows theoretical curves P_d/P_{fa} for different SNR (signal-to-noise ratio) varying from 10 to 50 dB, and the Fig. 5 represents the curves derived by simulation and Padé approximations. To simulate K -distributed processes we use the elegant SIRP theory (spherically invariant random process, [8,9]) which states that K -distribution ($\mathbf{X} = \mathbf{ZS}$) is derived with Gaussian vector (\mathbf{Z}) whose standard deviation is itself a gamma random variate (S), independent of \mathbf{Z} with a non-negative PDF $f_S(S)$ so-called the characteristic PDF of the SIRV (vector). This representation is interesting to take into account the possible noise correlation since a SIRV is invariant

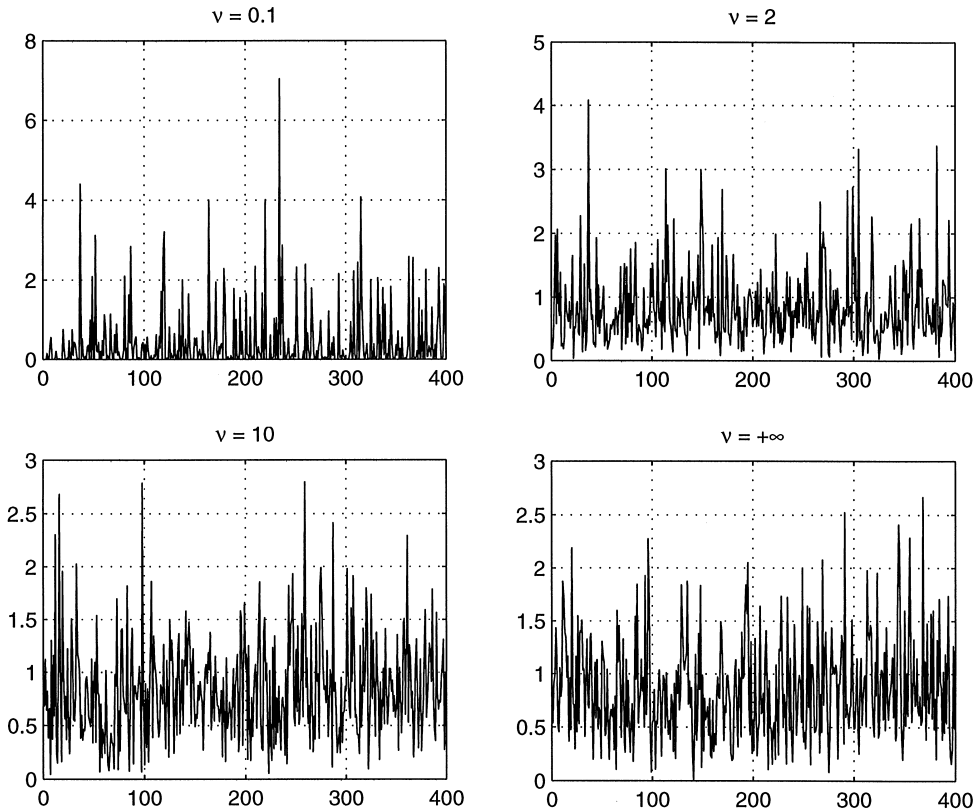


Fig. 3. Realizations of K -distributed noises for different values of $\nu = 0.1, 2, 10, +\infty$, power $\sigma^2 = 1$.

under linear transformation, that is to say that if \mathbf{X} is a SIRV then $\mathbf{Y} = \mathbf{A}\mathbf{X} + \mathbf{B}$ is a SIRV with the same characteristic PDF (\mathbf{A} is a non-singular matrix and \mathbf{B} is a vector having the same dimension as \mathbf{X}).

The Rayleigh probability law is the well-known Gaussian complex vector envelope law. The fluctuations coefficients $\{\gamma_i\}$ and $\{\delta_i\}$ are derived once for $A_0^2 = 1$ and then its law is deduced for each value of the SNR from the reference ($A_0^2 = 1$). The results show the excellent quality of the approximation.

5.2. Experimental data

The signal here analysed corresponds to experimental forest clutter data envelope spatially collected at low grazing angle ($< 1^\circ$) in 246 range bins of 0.5 m with an X-band radar. The aim of this

measurements campaign was to study ground clutter scatterers and we use few of them to evaluate the radar detection performances of a virtual target embedded in such an environment with the use of a Padé approximation on the noise envelope. For convenience, the noise power has been normalized to one.

Fig. 6 shows results of PDF and CDF Padé approximation of this experimental clutter data. Fig. 7 gives detection performances of a *hypothetical* non-fluctuating target which would be embedded (in phase and amplitude) in such a noise. The curves show the mismatch between real and Rayleigh hypothesis. For the latter, we can see on the curve that the false alarm rate increases until $P_{fa} = 1.34 \times 10^{-4}$ if we consider the true statistic of the analysed clutter.

The moments have been estimated from the set of complex clutter data y_i according to the

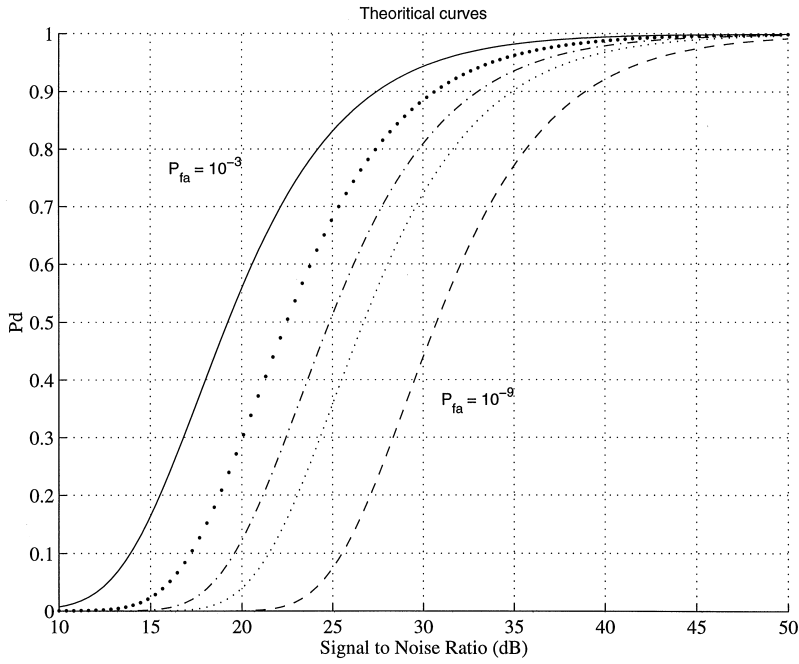


Fig. 4. Theoretical detection curves for $P_{fa} = 10^{-3}, 10^{-4}, 10^{-5}, 10^{-6}, 10^{-9}$: Swerling I fluctuating target embedded in K -distributed noise ($\nu = 0.1$ and $\sigma^2 = 1$).

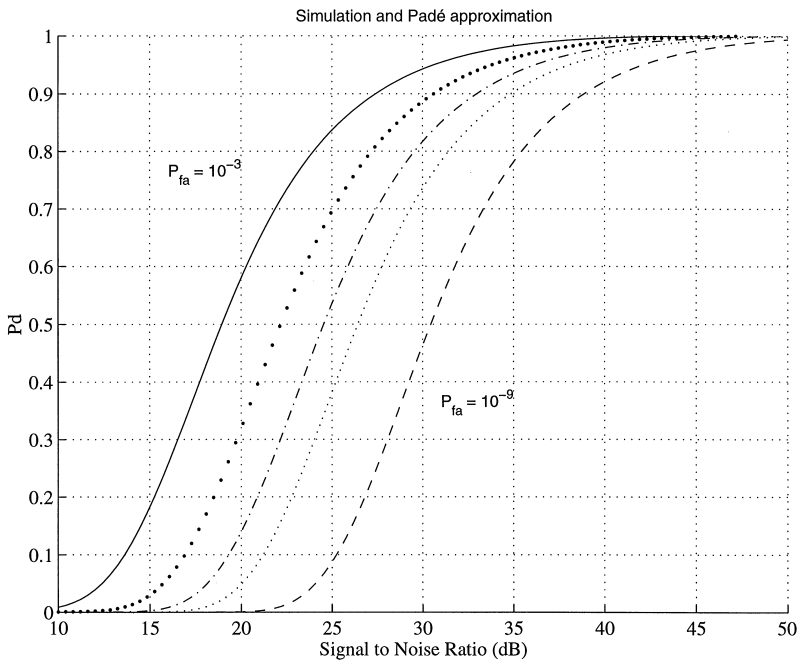


Fig. 5. Detection curves for $P_{fa} = 10^{-3}, 10^{-4}, 10^{-5}, 10^{-6}, 10^{-9}$: simulation and Padé approximation ($M = 4$): Swerling I fluctuating target embedded in K -distributed noise ($\nu = 0.1$ and $\sigma^2 = 1$).

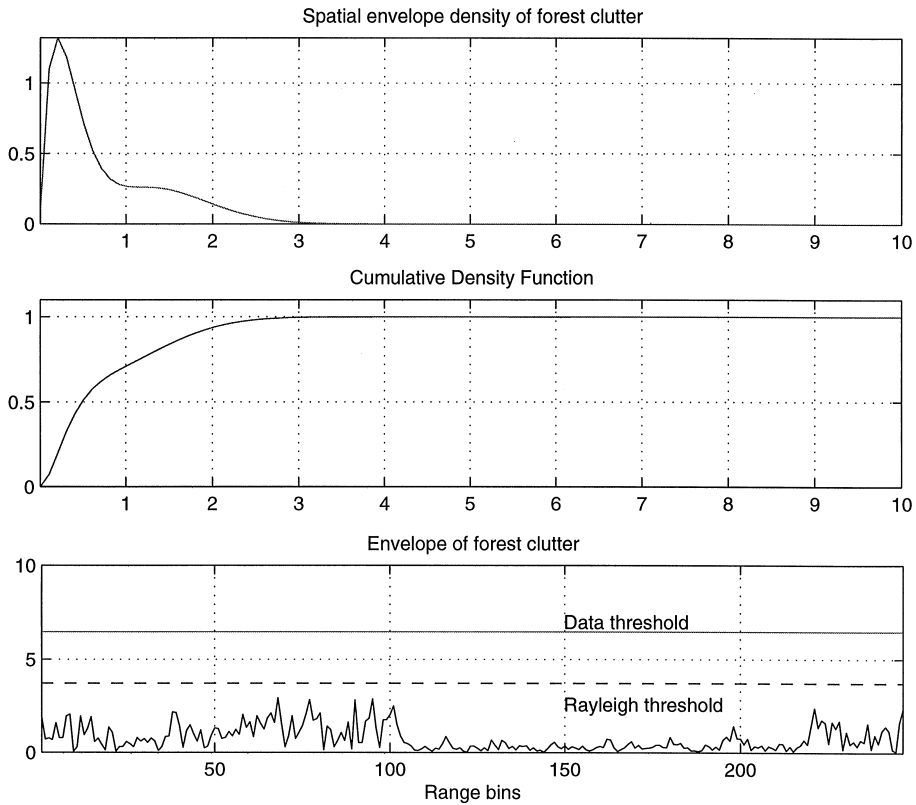


Fig. 6. Results of the approximation density obtained on the envelope of experimental data (forest clutter). The detection threshold θ for experimental data is calculated according to equation (39) with $P_{fa} = 10^{-6}$ and it has to be compared with the one computed for the Rayleigh hypothesis case.

classical way:

$$\hat{\mu}_n = \frac{1}{N} \sum_{i=1}^N |y_i|^n. \tag{50}$$

Asymptotically, it can be shown that $\hat{\mu}_n$ tends to the real values $\mathbb{E}(|y|^n)$ of the moments as $N \rightarrow \infty$ (where $\mathbb{E}(\cdot)$ denotes the mathematical expectation). Larger will be the number of data and better will be this estimation.

The normalised MGF of experimental data takes the form

$$\begin{aligned} \Phi(u) = & 1 - 0.7652u + 0.5u^2 - 0.2877u^3 \\ & + 0.1431u^4 - 0.06229u^5 + 0.02408u^6 \\ & - 0.008382u^7 + 0.00265u^8 - 0.0007672u^9 \\ & + 0.0002043u^{10} - 0.0000503u^{11} \end{aligned}$$

and the [5/6] Padé approximation becomes

$$P^{[5/6]}(u) = \sum_{k=1}^6 \frac{\lambda_k}{u - \alpha_k} \tag{51}$$

with

$$\begin{aligned} \{\lambda_k\}_{k \in [1,6]} = & \{8.4237 \pm 10.244i, \dots \\ & - 0.035157 \pm 0.038976i, \dots \\ & - 8.953 \pm 48.34i\} \end{aligned} \tag{52}$$

$$\begin{aligned} \{\alpha_k\}_{k \in [1,6]} = & \{- 2.823 \pm 1.9382i, \dots \\ & - 1.2425 \pm 3.153i, \dots \\ & - 3.2174 \pm 0.63591i\}. \end{aligned} \tag{53}$$

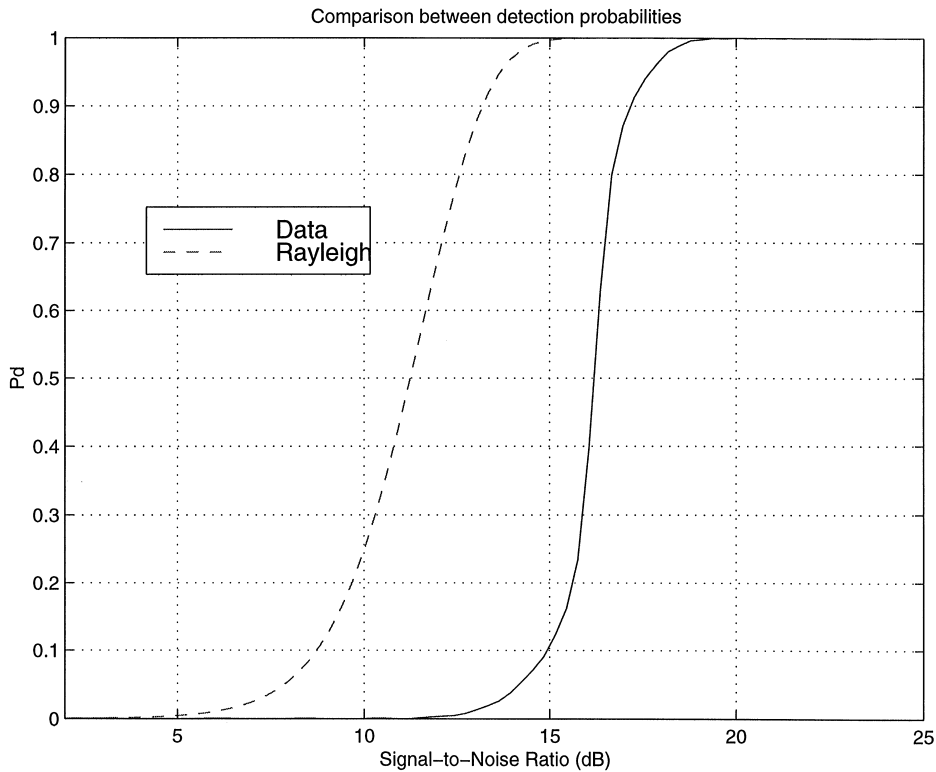


Fig. 7. Comparison between detection performances in experimental data (forest clutter) and detection performances in classical Rayleigh noise. The two noise signals have the same power and the results are shown for a probability of false alarm rate fixed to $P_{fa} = 10^{-6}$.

The last graphic on Fig. 6 shows the mismatch between the detection threshold values derived, the real one, $\theta_1 = 6.47$, by the resolution of (39), and the other, $\theta_2 = 3.71$, with the classical Gaussian hypothesis.

6. Conclusion

This paper has recalled a general modelisation method with few parameters of the true PDF of a complex process from a power series expansion of its MGF. This recalls the AR and ARMA spectral density modelisation methods and allows to derive simple and general relations of the pair (P_d, P_{fa}) . This method needs the knowledge to a high degree of accuracy of the n -order moments of the envelope of the unwanted noise often unavailable. We do not solve this problem in this paper either assuming

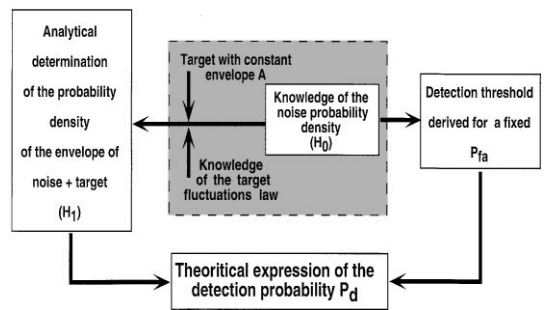


Fig. 8. Classical scheme to analyse the detection performances.

they are known or simulating a large number of variates in order to asymptotically tend to the real values. A study of the influence of an error on the moments estimation is currently investigated in further works.

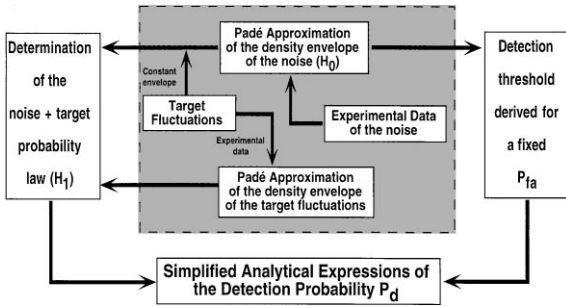


Fig. 9. Applying Padé approximation.

However, as we show in this work, Padé approximation method gives powerful expressions for a computational aid and allows to evaluate successfully, for instance, the detection performance analysis without a priori knowledge on the noise statistic.

As a conclusion to this paper and to show the difference between the classical detection way and the use of the Padé approximation we present two schemes (Fig. 8 for the classical way; Fig. 9 for the use of Padé approximation) resuming the two different approaches.

References

- [1] M. Abramowitz, I.A. Stegun, Handbook of Mathematical Functions, National Bureau of Standard, AMS 55 (June 1964).
- [2] H. Amindavar, Applications of Padé approximations in signal analysis, UMI Dissertations Services, Ph.D., University of Washington, 1991.
- [3] H. Amindavar, J.A. Ritcey, Padé approximations for detectability in K -clutter and noise, Proc. IEEE Trans.-AES 30 (2) (April 1994) 424–434.
- [4] H. Amindavar, J.A. Ritcey, Padé approximations of probability density functions, Proc. IEEE Trans.-AES 30 (2) (April 1994) 416–424.
- [5] J.B. Billingsley, Ground clutter measurements for surface-sited radar, Technical Report 780, MIT, February 1993.
- [6] E. Jakeman, R.J.A. Tough, Generalized K -distribution: a statistical model for weak scattering, J. Opt. Soc. Am. A 4 (9) (September 1987), 1764–1772.
- [7] J.P. Ovarlez, E. Jay, New methods of radar detection performances analysis, Proc. IEEE-ICASSP99, Phoenix, USA, March 1999.
- [8] M. Rangaswamy, D. Weiner, A. Öztürk, Computer generation of correlated non-Gaussian radar clutter, Proc. IEEE Trans.-AES 31 (1) (January 1995) 106–116.
- [9] M. Rangaswamy, D. Weiner, A. Öztürk, Non-Gaussian random vector identification using spherically invariant random processes, Proc. IEEE Trans.-AES 29 (1) (January 1993) 111–123.
- [10] B.W. Silverman, Density Estimation For Statistics and Data Analysis, Chapman & Hall, London, 1986.